1975

Thermal Instability in Supernova Shells

R. McCray
University pf Colorado

R. F. Stein
NASA, Goddard Space Flight Center

Menas Kafatos
Chapman University, kafatos@chapman.edu

Recommended Citation
McCray, R., Stein, R.F., Kafatos, M. (1975) Thermal Instability in Supernova Shells,*Astrophysical Journal*, 196: 565-570. doi: 10.1086/153436

Thermal Instability in Supernova Shells

THE ASTROPHYSICAL JOURNAL, 196:565–570, 1975 March 1

THERMAL INSTABILITY IN SUPERNOVA SHELLS

RICHARD MCCRAY* AND ROBERT F. STEIN†
Joint Institute for Laboratory Astrophysics, University of Colorado and National Bureau of Standards
AND
MINAS KAFATOS‡
Laboratory for Solar Physics and Astrophysics, NASA–Goddard Space Flight Center
Received 1974 August 12; revised 1974 September 16

ABSTRACT

Thermal instability in the radiative cooling region behind a shock will cause upstream density fluctuations to collapse into thin sheets aligned parallel to the shock front. A linearized calculation demonstrates the development of this instability. Thermal conduction suppresses the development of small-scale perturbations. Estimates of the scale sizes for the fully developed condensations agree roughly with the scale sizes of fine structure observed in supernova shells such as the Cygnus Loop.

Subject headings: gas dynamics — supernova remnants

I. INTRODUCTION

When the blast wave from a supernova explosion has reached a radius at which radiative cooling of the shocked gas can dissipate a significant fraction of the energy of the blast, a dense shell of gas forms behind the shock. The development of the shell has been described by Cox (1972*a*, *b*, *c*), Rosenberg and Scheuer (1973), Chevalier (1974), Straka (1974), and Mansfield and Salpeter (1974). Presumably, this shell is what we see in the photographs of supernova remnants—for example, the Cygnus Loop, the Vela supernova remnant, or Shajn 147 (cf. van den Bergh, Marscher, and Terzian 1973). These photographs also show beautiful lacy structure in the shells that has not been predicted by the calculations up to now. Evidently, the structure is one of multiple sheets of dense gas oriented parallel to the shock front and seen edge-on. Here we present a theory which shows that this lacy structure is the result of thermal instability in the cooling region behind the shock.

The mechanism of thermal instability was first described correctly by Field (1965). If a gas cools radiatively by binary atomic encounters in an optically thin gas, the cooling rate per particle can be written as $n\Lambda(T)$ (ergs s^{-1}), where n (cm^{-3}) is the proton density. (Strictly speaking, this is an approximation that only holds in the steady-state limit; however, Kafatos [1973] has shown that time-dependent cooling can be approximated reasonably well by a function of this type.) A dense region of gas cools more rapidly than its rarefied surroundings, and the propensity of the gas to approach pressure equilibrium may cause a runaway collapse of the dense region. In a gas with small spatial density fluctuations which is cooling from an elevated temperature, the condition for the development of such an instability is that the logarithmic slope of the cooling function $S \equiv d \log \Lambda / d \log T < 2$ (Field 1965). The development of such an instability has been described in detail by Schwarz, McCray, and Stein (1972).

In a supernova shell, the gas behind the shock is not uniform in space or in time, so the analysis of its stability is more complicated. Mufson (1974) has discussed thermal instability of a galactic spiral-arm shock in a multiphase model for the interstellar medium. Our method of analysis differs from Mufson's, because the physics of the supernova shell problem is different and we wish to emphasize different observational consequences.

The basic equations are (cf. Field 1965):

$$\frac{dn}{dt} + n\nabla\cdot v = 0\,, \tag{1}$$

$$n\mu \frac{dv}{dt} + \nabla p = 0\,, \tag{2}$$

$$\frac{1}{\gamma - 1}\frac{dp}{dt} - \frac{\gamma}{\gamma - 1}\frac{p}{n}\frac{dn}{dt} + n^2\Lambda(T) - \nabla\cdot(K\nabla T) = 0 \tag{3}$$

and

$$p - n'kT = 0\,, \tag{4}$$

where $d/dt = \partial/\partial t + v\cdot\nabla$, $K(T)$ is the coefficient of thermal conductivity, μ is the mean molecular weight per proton, n' is the free particle density, and γ is the ratio of specific heats. Viscosity is negligible, and in the analysis following we shall drop the thermal conductivity term. The importance of these effects and others (e.g., magnetic pressure) will be discussed later.

We make the idealization, following Cox (1972*a*), of ignoring curvature and deceleration of the shock front, so that the unperturbed shock structure is a steady

* Also Department of Physics and Astrophysics, University of Colorado.

† JILA Visiting Fellow, on leave from Department of Physics, Brandeis University.

‡ NRC-NAS Resident Research Associate.

one-dimensional flow described by proton density $n_0(x)$, velocity $v_0(x)$, temperature $T_0(x)$, and pressure $p_0(x)$. We assume that the upstream pressure is negligible (very strong shock). Equations (1)–(4) then yield, for steady flow:

$$n_0 v_0 = NV , \tag{5}$$

$$p_0 + \mu n_0 v_0^2 = \mu N V^2 , \tag{6}$$

$$v_0 \frac{d}{dx}\left[\frac{\gamma}{\gamma - 1}\frac{p_0}{n_0} + \tfrac{1}{2}\mu v_0^2\right] + n_0 \Lambda(T_0) = 0 , \tag{7}$$

where N is the upstream proton density and V is the shock velocity. We define a density ratio $u = n_0(x)/N = V/v_0(x)$, so that

$$T_0(u) = \frac{\mu n_0 V^2}{n' k}\left(\frac{1}{u} - \frac{1}{u^2}\right) , \tag{8}$$

and

$$p_0(u) = n' k T_0(u) .$$

The actual shock front in which the velocity distribution function is isotropized is assumed to be very thin compared with the characteristic cooling length. This should be true for the highly ionized gas in supernova shells, where plasma streaming instabilities are probably much more effective than particle collisions (Zel'dovich and Raizer 1967). Therefore we have $u_1 = (\gamma + 1)/(\gamma - 1)$ ($u_1 = 4$ for $\gamma = 5/3$), where the subscript 1 indicates the value of the variable immediately behind the shock.

We define a characteristic cooling length

$$L_1 = \frac{\mu v_1^3}{(\gamma - 1) n_1 \Lambda(T_1)} = \frac{\mu V^3}{(\gamma - 1) u_1^4 N \Lambda(T_1)} . \tag{9}$$

The solution of equation (7) can then be written

$$x(u) = L_1 \int_{u_1}^{u} \left(\frac{u_1}{u}\right)^4 [\gamma - (\gamma + 1)/u] \frac{\Lambda(T_1)}{\Lambda(T_0)}\, du , \tag{10}$$

where T_0 and T_1 are related to u and u_1 by equation (8).

As a specific illustration, consider a shock moving with velocity $V = 100$ km s^{-1} into a medium of hydrogen density $N = 1$ cm^{-3} and cosmic abundances. The upstream gas is assumed to be photoionized by radiation from the shock. Then $\gamma = 5/3$, $u_1 = 4$, $n'/n = (2n_{\rm H} + 3n_{\rm He})/n_{\rm H} = 2.3$, $\mu = 1.4 m_{\rm H}$, and $T_1 = 1.37 \times 10^5$ ° K. The time-dependent radiative cooling function has been calculated by Kafatos (1973). A good fit over the temperature range 10^4 ° K $< T < 10^6$ ° K is given by

$$\Lambda(T) = 5 \times 10^{-22} \exp(-5 \times 10^4 \text{ ° K}/T) \text{ ergs cm}^3 \text{ s}^{-1} , \tag{11}$$

so that $S = 5 \times 10^4$ ° K/T, and, by equation (9), $L_1 = 3.9 \times 10^{16}$ cm. This solution to equation (10) with the given parameters is shown as curve (*a*) of figure 1. It agrees fairly well with the corresponding solution given by Cox (1972*a*) who used slightly different abundances and cooling rates, except that our solution does not have the temperature falling much below 10^4 ° K because our cooling function does not include any trace-element cooling below 10^4 ° K. The main qualitative property of the solution of figure 1 is the collapse of the gas to high density and low temperature in such a way that approximate pressure equilibrium is maintained in the cooling region behind the shock. (The temperature T varies approximately as $1/n$.)

Now suppose that the shock is moving into a region

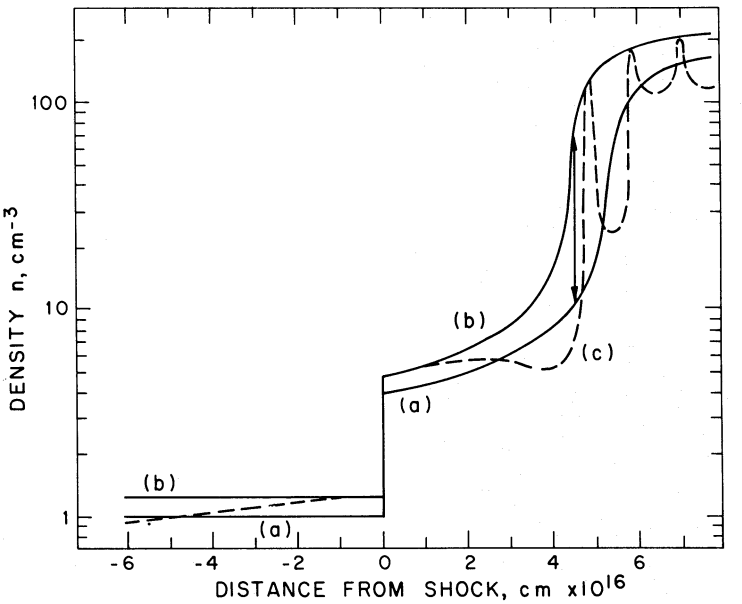

FIG. 1.—Gas density in a radiatively cooling shock. (*a*) Uniform upstream density $N = 1.0$ cm^{-3}. (*b*) Uniform upstream density $N = 1.2$ cm^{-3}. (*c*) Sinusoidal upstream density variation.

of variable density. The effect of increasing N is to reduce the scale length L_1, so that the location of the thermal collapse is closer to the shock front. This is illustrated by curve (b) of figure 1, which is the corresponding solution to equation (10) with an upstream density 20 percent greater, $N = 1.2\ \mathrm{cm}^{-3}$. The upstream density fluctuation is reflected as a much greater density fluctuation at a fixed distance from the shock, as indicated by the arrow which shows an (8:1) density fluctuation in the collapsing region.

The condition for large amplification of an incoming density fluctuation is related to the logarithmic slope S of the cooling function. It can be derived in a simple way by taking $\Lambda(T) \propto T^S$. Then an approximation to the downstream structure is obtained by neglecting terms $\sim 1/u$ in equation (10), which yields

$$x(u) \approx \frac{L_1 \gamma \mu_1}{3 - S}\left[1 - \left(\frac{u_1}{u}\right)^{3-S}\right]. \tag{12}$$

Equation (12) shows that if $S < 3$ the cooling region behind the shock will collapse to infinite density in a finite distance. Now suppose the shock enters a region where the upstream density has a fluctuation $N \rightarrow N + \delta N$. This fluctuation shows up as a density fluctuation δn in the downstream cooling region, related to δN by

$$\left(\frac{\delta \log n}{\delta \log N}\right)_{x,V} \approx 1 + \left(\frac{u}{u_1}\right)^{3-S} \frac{x}{L_1 \gamma u_1}. \tag{13}$$

Equation (13) shows that if $S < 3$, an upstream density fluctuation will be amplified by a large factor in the collapsing region.

II. LINEAR ANALYSIS

The above considerations only apply directly to incoming density fluctuations with upstream wavelength $\lambda \gg L_1$. In order to understand better how the amplification process depends on the wavelength of the incoming fluctuations, we make a linear perturbation analysis of the fluid equations (1)–(4). It is convenient to express the fluid variables in terms of the unperturbed variables as follows:

$$\begin{aligned} n(x, t) &= n_0(x)[1 + \tilde{n}(x)e^{i\omega t}], \\ v(x, t) &= v_0(x)[1 + \tilde{v}(x)e^{i\omega t}], \\ p(x, t) &= p_0(x)[1 + \tilde{p}(x)e^{i\omega t}], \end{aligned} \tag{14}$$

where $\tilde{n}(x)$, $\tilde{v}(x)$, and $\tilde{p}(x)$ are complex dimensionless variables describing the first-order fractional perturbations. It is then a straightforward though lengthy exercise in algebra to substitute expressions (14) into equations (1)–(4), retaining only first-order terms, and derive differential equations for $\tilde{n}(x)$, $\tilde{v}(x)$, and $\tilde{p}(x)$. Equations (5)–(7) are used to express the zero-order variables $n_0(x)$, $v_0(x)$, $p_0(x)$, and their derivatives in terms of $u(x) = n_0(x)/N$. For purposes of computation it is convenient to change the dependent variable from x to u by means of equation (10). The net result of all these operations is a set of equations that can be written in matrix form as

$$\frac{d}{d \ln u}\begin{pmatrix} \tilde{n}(u) \\ \tilde{v}(u) \\ \tilde{p}(u) \end{pmatrix} = M_{ij}\begin{pmatrix} \tilde{n}(u) \\ \tilde{v}(u) \\ \tilde{p}(u) \end{pmatrix}, \tag{15}$$

where

$$\begin{aligned} M_{11} &= \left[\frac{2\alpha - 1}{\alpha - 1} - S\right] - i\delta \frac{\alpha - 1}{\tilde{\Lambda}(u)}\left(\frac{u_1}{u}\right)^3, \\ M_{12} &= -\left[\frac{\alpha - 3}{\alpha - 1}\right] - i\delta \frac{1}{\tilde{\Lambda}(u)}\left(\frac{u_1}{u}\right)^3, \\ M_{13} &= -\left[\frac{\alpha}{\alpha - 1} - S\right] + i\delta \frac{u - 1}{\tilde{\Lambda}(u)}\left(\frac{u_1}{u}\right)^3, \\ M_{21} &= -\left[\frac{2\alpha - 1}{\alpha - 1} - S\right], \\ M_{22} &= -M_{12}, \qquad M_{23} = -M_{13}, \\ M_{31} &= \left[\frac{3\alpha - 2}{\alpha - 1} - S\right]\frac{1}{(u - 1)}, \\ M_{32} &= \left[\frac{\alpha + 1}{\alpha - 1}\right]\frac{1}{(u - 1)} - i\delta \frac{\gamma}{\tilde{\Lambda}(u)}\left(\frac{u_1}{u}\right)^3, \\ M_{33} &= -\left[\frac{2\alpha - 1}{\alpha - 1} - S\right]\frac{1}{(u - 1)} + i\delta \frac{1}{\tilde{\Lambda}(u)}\left(\frac{u_1}{u}\right)^3, \end{aligned}$$

and we have made the following definitions:

$$\alpha \equiv \gamma(u - 1),$$

$$\tilde{\Lambda}(u) \equiv \frac{\Lambda[T_0(u)]}{\Lambda[T_0(u_1)]},$$

and

$$\delta \equiv \frac{\omega L_1 u_1}{V} \tag{16}$$

is the ratio of the cooling distance to the wavelength of the perturbation immediately behind the shock.

One may recover the asymptotic behavior (13) by taking the long-wavelength limit $\delta = 0$ in equation (15). Then, if $S < 2$ the equations have approximate analytic solutions in the limit $u \gg 1$ as follows: $\tilde{p}(u) \rightarrow 0$, $\tilde{n}(u) + \tilde{v}(u) \rightarrow$ const., and $\tilde{n}(u) \propto u^{3-S}$.

In order to represent a shock with constant driving pressure moving into a region of variable density, we choose as initial conditions $\tilde{n} = 1$, $\tilde{v} = -\frac{1}{2}$, $\tilde{p} = 0$ at $x = 0$ (so that $p \propto \mu n v^2 \approx$ constant, cf. eq. [8], and the shock front slows down a little as it enters a density enhancement). Of course, the magnitude of $\tilde{n}$ is irrelevant in the linearized theory; only the fractional change is significant.

Equations (15) have been integrated numerically, using parameters $N = 1\ \mathrm{cm}^{-3}$, $V = 100\ \mathrm{km\ s}^{-1}$, and the cooling function (11), as in figure 1. The results are given in figure 2, which shows the amplitude $|\tilde{n}|$ of the

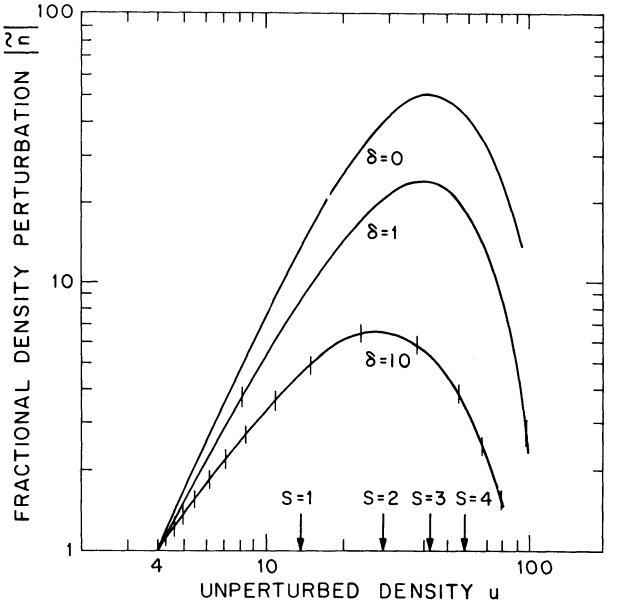

FIG. 2.—Growth of fractional density perturbation for various values of upstream wavelength. Logarithmic slope S of radiative cooling function is noted.

relative density fluctuation as a function of the unperturbed density $u = n(x)/N$. Curves are shown for $\delta = 0$, $\delta = 1.0$, and $\delta = 10.0$, which correspond to upstream wavelengths ∞, 9.9×10^{17} cm, and 9.9×10^{16} cm, respectively, according to equation (16). The tick marks on the curves show the nodes Re $(\tilde{n}) = 0$. The values of u for which $S = 1, 2, 3, 4$ are also marked.

In each case the density fluctuation grows in the cooling region for $S < 2$, reaches a maximum where $2 < S < 3$ ($28 < u < 43$), and decreases rapidly for $S > 3$. The maximum density fluctuation has the value $|\tilde{n}| = 50$ for $\delta = 0$, $|\tilde{n}| = 22.7$ for $\delta = 1$, and $|\tilde{n}| = 6.72$ for $\delta = 10$. Despite the considerable growth of the density fluctuation in each case, the pressure fluctuation $|\tilde{p}|$ never exceeds 1.4 and is usually of order 0.2. This result supports the assumption that the shock moves as if it is driven by constant pressure.

These results do not depend strongly on initial conditions. For instance, if we choose instead initial conditions appropriate to a constant velocity shock moving into a region of variable density, $\tilde{n} = 1$, $\tilde{v} = 0$, $\tilde{p} = 1$, we find that the shorter-wavelength perturbations initially damp out, and do not reach as great a maximum (the maximum values of $|\tilde{n}|$ are then 27, 4.7, 3.3, for $\delta = 0$, 1, 10, respectively). This can be understood because the initial perturbations, having elevated pressure, tend to expand freely at first. However, the initial conditions $\tilde{n} = 1$, $\tilde{v} = -\frac{1}{2}$, $\tilde{p} = 0$ are more appropriate.

With higher shock velocities than in the example above, the instability mechanism is still effective, and perturbations with even longer upstream wavelengths will collapse to filaments. (A more accurate radiative cooling function given by Kafatos [1973] shows that $S < 0$ for $T \gtrsim 2 \times 10^5$ ° K.) In fact the thermal instability becomes effective as soon as the supernova shell reaches the cooling stage with $V \lesssim 300$ km s^{-1} and $T_1 \lesssim 10^6$ ° K (cf. Cox 1972*b*), and remains effective until $S > 2$ ($T < 2.5 \times 10^4$ ° K).

III. DISCUSSION

We now discuss the meaning of these results and the interpretation of fine structure in supernova shells. First, it is clear from figures 1 and 2 that small incoming density fluctuations may be amplified by a large factor at a distance $\sim L_1$ behind the shock. The maximum amplification decreases for incoming fluctuations of upstream scale size $\lesssim 10L_1$ ($\delta \gtrsim 1$), but is still significant for shorter wavelengths. We have not done nonlinear calculations, but we can guess what the ultimate fate of the condensations will be, using simple physical arguments that have been borne out by other nonlinear calculations (cf. Schwarz *et al.* 1972). The condensations will continue to collapse and cool until radiative cooling shuts off, in such a way that approximate pressure equilibrium is maintained between condensations and the surrounding gas. The nonlinear development of the condensations will proceed more rapidly than indicated by the linearized theory once $|\tilde{n}| \gtrsim 0.3$. When the cooling shuts off, the condensations cease to collapse but the surrounding hot gas continues to cool radiatively. The dense condensations then begin to expand again and dissipate, as indicated by the linear theory (cf. fig. 2) which shows the perturbations damping rapidly when $S > 3$.

The maximum density contrast can be estimated by the pressure equality condition $n_1 T_1 = n_{\max} T_{\min}$, where $T_{\min}$ is the temperature at which the radiative cooling shuts off. For the example chosen, $T_1 = 1.37 \times 10^5$ ° K, and the radiative cooling function (11) shuts off effectively at $T_{\min} \approx 8000$° K, so that the downstream density contrast may reach ~ 17.

The nonlinear development of density fluctuations is illustrated schematically by the dashed curve (*c*) of figure 1. A density fluctuation entering the shock has its scale length compressed first by a factor 4 in the adiabatic shock. Then it is further compressed by a factor ~ 17 by the thermal instability. Therefore, the net compression along the flow direction is ~ 70. If an incoming condensation has roughly equal dimensions parallel and perpendicular to the shock, we would expect it to become a sheetlike structure with transverse dimensions ~ 70 times greater than its thickness.

We consider as an example the Cygnus Loop, and assume a distance $D \approx 770$ pc and the parameters of figure 1, following Cox (1972*a*). The cooling distance $L_1 = 3.9 \times 10^{16}$ cm then corresponds to an angular dimension $\sim 4''$. Highly magnified photographs of portions of the Cygnus Loop (cf. Miller 1974), for example, show a network of roughly parallel striations —"filaments"—typically separated by a few arc seconds. Evidently these filaments are sheets seen edge-on. Further, the typical lengths of these filaments are of order a few arc minutes, which suggests a

compression by roughly a factor 60. A length of a few arc minutes suggests that we are looking at the result of compression of interstellar condensations that have initial diameters of a few tenths of parsecs. Such fine structure in interstellar H I was predicted by Schwarz *et al.* (1972). It is difficult to observe, but recently Greisen (1973), using 21-cm absorption interferometry, has seen indications of structure on scales ~ 0.14 pc.

The numbers suggested here for the Cygnus Loop are merely representative; a detailed application of the theory to the observed filamentary structure would require better knowledge of the parameters of the shock than we now have. For example, Cox (1972*a*, *c*) suggests values $N = 6\ \mathrm{cm}^{-3}$, $V = 100\ \mathrm{km\ s}^{-1}$ to account for the optical emission of the brighter filaments. This would imply $L_1/D \approx 0''.6$, too small to be resolved. However, the X-ray map of Rappaport *et al.* (1974) shows that the soft X-rays come from the same regions where the bright optical filaments are located, and the gas temperature $T \approx 2.9 \times 10^6\ ^\circ\mathrm{K}$ inferred from the soft X-ray spectrum implies a shock velocity $V \approx 450\ \mathrm{km\ s}^{-1}$. If the soft X-rays resulted from a spherically symmetric blast wave entering an ambient medium of density N, the observed soft X-ray flux from the entire Loop implies $N \approx 0.25\ \mathrm{cm}^{-3}$ (cf. Gorenstein, Harnden, and Tucker 1974), but the gas density is obviously not uniform around the Loop. The brighter X-ray emitting regions might well have $N \approx 10\ \mathrm{cm}^{-3}$, $V \approx 450\ \mathrm{km\ s}^{-1}$, giving $L_1/D \approx 20''$, of the same order of magnitude as the separation of the filaments.

The development of the condensations after their temperature drops below 8000° K is uncertain. In the above analysis we have assumed that the condensations are optically thin to the emitted radiation. This is a good assumption for the high-temperature gas, but when the temperature drops below 8000° K and the hydrogen recombines significantly, the heating due to photoabsorption of radiation from the hotter gas is comparable to the radiative cooling. Perhaps the heating is strong enough to prevent the sheets from cooling and collapsing further, so that they expand again and dissipate as suggested above. Alternatively, there may be enough radiative cooling below 8000° K that the thermal collapse continues (cf. Cox 1972*a*). This question is not material to the observations, though, because when the temperature drops below $\sim 5000^\circ$ K the gas ceases to emit the strong optical lines by which we observe the filaments. In fact, the optical emissivity of the gas is such that the filaments are most easily observable at precisely the time when the density contrast is $\sim 70{:}1$.

Various effects modify the development of the thermal instability described here. For example, magnetic pressure may limit the development of dense filaments if the field is aligned parallel to the shock front. To estimate this effect, we assume that the frozen-in magnetic field is compressed in one dimension perpendicular to the shock front, and set the gas pressure immediately behind the shock equal to that of the compressed field:

$$3/4 N \mu V^2 = \left(\frac{n_{\max} B_0}{N}\right)^2 \Big/ 8\pi\,. \tag{17}$$

Therefore, with a typical interstellar magnetic field $B_0 = 3 \times 10^{-6}$ gauss, $N = 1\ \mathrm{cm}^{-3}$, $V = 100\ \mathrm{km\ s}^{-1}$, we find $n_{\max}/N \approx 20$, instead of ≈ 70 with $B_0 = 0$. However, if the magnetic field is not aligned nearly parallel to the shock, the development of the thermal instability will probably not be limited by magnetic pressure; instead, the dense sheets will tend to align perpendicular to the magnetic field.

Thermal conduction will suppress the growth of perturbations of short wavelength. To estimate this effect, we approximate the conductivity term in equation (3) by KT/L^2, where L is the scale length of the fluctuation, and set the rate of radiative cooling equal to the rate of conductive heating to obtain a critical scale length:

$$L_c \approx \left(\frac{KT}{n^2 \Lambda(T)}\right)^{1/2}. \tag{18}$$

Perturbations of scale length $L \lesssim L_c$ will be damped by thermal conduction. The appropriate thermal conductivity for the situation under consideration is that for a fully ionized gas (Spitzer 1962), $K = 1.2 \times 10^{-6}\ T^{5/2}\ \mathrm{ergs\ cm}^{-1}\ \mathrm{s}^{-1}\ (^\circ\mathrm{K})^{-1}$. We then find for the ratio of L_c to the cooling length L_1 (eq. [9]),

$$\frac{L_c}{L_1} \approx 0.3 (T/10^5\ ^\circ\mathrm{K})^{1/4} \exp\left(-2.5 \times 10^4/T\right), \tag{19}$$

where we have used the cooling function (11). Equation (19) shows that thermal conduction will prevent the collapse of fluctuations of scale length $\lesssim 0.3\, L_1$, or upstream wavelength $\lesssim L_1$, considering the 4:1 adiabatic compression at the shock.

We believe that the simplified one-dimensional analysis presented here is sufficient to demonstrate that thermal instability in a radiatively cooling shock is responsible for the fine structure in supernova shells. Of course, the observed structure is the result of nonlinear amplification, and is no doubt modified by two-dimensional effects such as the bending of shocks around density fluctuations and oblique magnetic fields. Two-dimensional numerical hydrodynamical simulations are required. Chevalier and Theys (1975) have made a good start in this direction; it will be very interesting to see the results of more detailed studies along these lines.

We acknowledge useful discussions with Dr. D. P. Cox.

This work was supported by NSF grant GP-38736. Computer time was provided by a grant from the National Center for Atmospheric Research which is sponsored by the National Science Foundation.

REFERENCES

Chevalier, R. A. 1974, *Ap. J.*, **188**, 501.
Chevalier, R. A., and Theys, J. C. 1975, *Ap. J.*, **195**, 53.
Cox, D. P. 1972*a*, *Ap. J.*, **178**, 143.
Cox, D. P., 1972*b*, *Ap. J.*, **178**, 159.
———. 1972*c*, *ibid.*, p. 169.
Field, G. B. 1965, *Ap. J.*, **142**, 531.

Gorenstein, P., Harnden, F. R. Jr., and Tucker, W. H. 1974, *Ap. J.*, **192**, 661.
Greisen, E. W. 1973, *Ap. J.*, **184**, 37.
Kafatos, M. 1973, *Ap. J.*, **182**, 433.
Mansfield, V. N., and Salpeter, E. E., 1974, *Ap. J.*, **190**, 305.
Miller, J. S., 1974, *Ap. J.*, **189**, 239.
Mufson, S. L. 1974, *Ap. J.*, **193**, 561.
Rappaport, S., Doxsey, R., Solinger, A., and Borken, R. 1974, *Ap. J.*, **194**, 329.
Rosenberg, I. and Scheuer, P. A. G. 1973, *M.N.R.A.S.*, **161**, 27.
Schwarz, J., McCray, R., and Stein, R. F. 1972, *Ap. J.*, **175**, 673.
Spitzer, L., 1962, *Physics of Fully Ionized Gases* (New York: Interscience).
Straka, W. C., 1974, *Ap. J.*, **190**, 59.
van den Bergh, S., Marscher, A. P., and Terzian, Y. 1973, *Ap. J. Suppl.*, **26**, 19.
Zel'dovich, Ya. B., and Raizer, Yu. B., 1967, *Physics of Shock Waves and High Temperature Hydrodynamic Phenomena*, Vol. **2**, ed. W. D. Hayes and R. F. Probstein (New York: Academic Press).

Minas Kafatos: Code 680, NASA—Goddard Space Flight Center, Greenbelt, MD 20771

Richard McCray: JILA, University of Colorado, Boulder, CO 80302

Robert F. Stein: Department of Physics, Brandeis University, Waltham, MA 02154